

GNSS NETWORK REAL TIME POSITIONING: TESTING PROCEDURE TO EVALUATE THE ACCURACY OF A GEODETIC MOVING ANTENNA

C. Gordini^a, C. Abbondanza^b and M. Barbarella^b

^a University of Melbourne, Department of Geomatics (cgordini@unimelb.edu.au)

^b Alma Mater Studiorum University of Bologna, DISTART Department
(claudio.abbondanza ; maurizio.barbarella)@mail.ing.unibo.it

KEY WORDS: Navigation, Network RTK, GNSS application, Least Square Estimation

ABSTRACT:

Academia, Industry and Government are investigating the reliability to use the real time kinematic (RTK) Global Navigation Satellite System (GNSS) techniques for centimetre level positioning of many existing and emerging applications. These include for instance mobile mapping and airborne laser scanning systems. The classical RTK methodology allows for an operational distance between the reference station and the user, within a range of 10-15 kilometres, due to the effect of correlation of some GNSS errors which tend to increase with distance. The adoption of a network-based RTK (NRTK) allow to extend centimetric level positioning within continuously operating reference station network (CORS) with separation distance up to 70 kilometres. One of the research aim was to evaluate the positional accuracy of the GNSS NRTK for mobile mapping applications. In order to understand the potentiality and the limitations of this methodology a testing procedure was designed using the BO-POS Network, established in 2003 in an area within Emilia-Romagna, Marche e Toscana. From an operational point of view, a double antenna system was mounted on board of a vehicle also equipped with three dual frequency receivers capable of NRTK positioning. In order to investigate the GNSS NRTK positional accuracy for mobile mapping system applications a least square-based algorithm was developed to determine a reference trajectory.

This paper describes the Bologna CORS network, the testing procedure adopted and details the algorithm based on a constrained least square adjustment of the phase centres' coordinates of the 2 antennae. The positional accuracy of the NRTK path will be finally assessed by comparing the results of the NRTK trajectory with post processed adjusted one.

1. INTRODUCTION

In many countries, permanent networks of continuously operating GNSS reference stations are now routinely used to support an increasing number and diversity of applications. These include traditional activities such as maintenance of the geodetic datum, land surveying and deformation monitoring where typically solutions available from post processing techniques are adequate. More recently however, applications such as road-cadastre, LIDAR (Barbarella and Gordini 2005), precision agriculture, machinery control and location based services are demanding centimetric level position solutions in real time. As such, these reference station networks can no longer only offer a passive service, where data are captured and archived, but must now deliver an active service through the computation and transmission of data to support real time kinematic GNSS operation.

As well known the traditional mode of high accuracy differential GPS (DGPS) positioning requires one GPS receiver to be located as a base station with known coordinates, while the second user receiver simultaneously tracks the same satellite signals. When the carrier phase measurements from the two receivers are combined and processed, the mobile user's receiver coordinates relative to the base receiver are determined. This can be done in real-time, if the reference receiver data are transmitted to the user's receiver, even while the receiver is moving (RTK). However, RTK GNSS positioning is limited by

the presence of systematic errors that degrade the accuracy of the solution as the distance away from an established reference station increases. To overcome this limitation, use of a solution generated using multiple reference stations has been proposed (Landau et al., 2003). Apart from relinquishing the dependency on a single reference station, this approach uses the networked stations to map regional atmospheric conditions (and other unmodelled double-differenced biases). This is significant as the baseline length over which the distance dependent errors are effectively eliminated with a single reference station is generally limited to 10-15 km (ICSM, 2004), especially when the ionosphere is active. The use of network-based techniques effectively extend the baseline length to support medium-range RTK operation, even up to 70 km or more in mid-latitude areas (Vollath et al., 2002, Rizos and Han 2002).

The philosophy underlying the use of a network of reference stations for accurate real time positioning allows to solve GNSS carrier phase ambiguities between the stations, once pre-determined coordinates for these stations have been used. Once this has been achieved, a significant portion of ionospheric, tropospheric, orbit and satellite clock biases can be estimated over a region and this information provided to a user in the field. As such the algorithms involved in generating network RTK solutions consist of three steps: network carrier phase ambiguity resolution epoch by epoch, bias estimation for each reference station and bias interpolation at the user location.

Using NRTK approach applications such as LIDAR, Direct Photogrammetry (Baldi et al., 1998), Road-Cadastral can map a wider area achieving cm or dm level of accuracy. It has been shown that cm level accuracy is achievable with inter-receiver distance between 40 and 70 km and 0.2m is achievable in sparse network with inter-receiver distance up to 155km (Gordini et al., 2006).

However different to the stationary case where a reference value for the positional accuracy evaluation is easily computable using long sessions of observation, for the kinematic real time data the computation of a reference trajectory is more critical (Al-Bajari 2000; Barbarella and Gordini 2005). A classical single baseline post processed solution for cm level positioning is limited to 15 km. Therefore to validate the accuracy of NRTK kinematic beyond this distance there is the need to build a 'true trajectory' to use as a reference. This study proposes a method based on a constrained least square adjustment to provide a true trajectory to validate NRTK data. In particular an investigation for validating the accuracy of network real time kinematic positioning, the procedure adopted and the practical results obtained using the BO-POS network will be presented.

2. CASE STUDY

2.1 The BO-POS Network for real time positioning

To test and evaluate the performance of a network RTK system, the DISTART Department of the University of Bologna initiated a pilot project in the Emilia Romagna region of Italy in July 2003 (Barbarella et al., 2003). Emilia Romagna is situated in the north of Italy, bordering with both the Lombardy and the Veneto regions in the north as well as Toscana and Marche in the south (Figure 1). The first phase of the project involved the establishment of a CORS test-bed network. The primary aim of this project was to evaluate the performance of these systems in terms of stability, reliability, integrity and accuracy.

In order to evaluate the performance of the system for centimetric positioning over longer distances, an inter-receiver distance extended to approximately 70-80 km was chosen. The CORS network currently operating in Emilia Romagna, has to fulfil several criteria in order to warrant the availability of a high level of security for the RS, a power supply, easy access to communication links (via internet connection), a good satellite visibility and a minimum presence of interferences to the GNSS signal. Public buildings such as universities and schools can usually satisfy the first three requirements. To verify the absence of possible interferences to the GNSS signal and local obstructions to satellite visibility, some tests were carried out in potential candidate sites. Each of the reference stations installed for this research consisted of a GNSS dual frequency receiver, a geodetic antenna, a com-server, an internet connection and a unit power supply (UPS). The computing centre was situated in Bologna and has started with GPSNet™ Trimble in 2003, GNSMART® software by GEO++® in 2004/2005 and Leica GPS Spider since the second part of 2005 (Barbarella et al., 2006). To make the system operative an intra-inter network between the reference stations, computing centre and user's station was established. Com server devices were adopted to connect each reference station with the internet provider with a serial and an Ethernet port respectively. These devices use stream binary transfer control protocols (TCP/IP) to communicate with the internet provider with a static internet protocol (IP) address. A Lantronix UDS 10-02 device, compatible with recommended standard RS 232 e RS 485/422 at 115.2 Kbps, was used for each reference station.

As mentioned above, to have a good estimation of the biases, it is necessary to correctly fix the network carrier phase ambiguity. For this purpose sub-centimetric knowledge of the reference station coordinates is required. Therefore, before starting the measurement field sessions the RS coordinates were calculated in post processing using Bernese v5.0 software. For this calculation, data collected in a one month session and final IGS precise satellite orbits were used. Mobile mapping applications often ask for a proper framing into the National Reference Frames. For this reason the whole BO-POS network was inserted into the National Geodetic Frame (IGM95). Therefore a GPS static session was undertaken on seven IGM95 mark points within the CORS network, whose coordinates were computed also into the ITRF2000 in such a way that it was possible to estimate the transformation parameters between the two frames (IGM95 and ITRF2000).

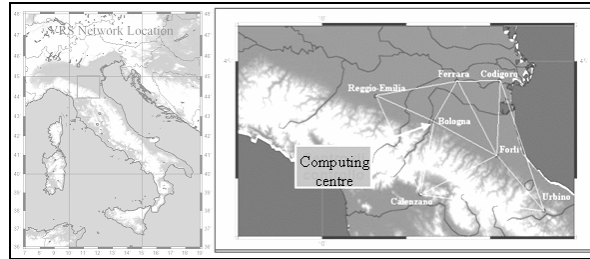


Figure 1. Area test

2.2 Network and software solution for this test

In this paper data collected with the GNSMART® software by GEO++® (Wübbena et al., 2001) are presented. The network configuration (Figure 2) consists of 7 reference stations: Bologna, Reggio Emilia, Forlì, Ferrara, Codigoro, Calenzano and Urbino with an average inter receiver distance of approximately 81km, which represents a fairly sparse network configuration; in fact the limit of 70 km is recommended from the GNSS manufactures (Trimble Navigation Limited, 2001). This software provides correction to the user's receiver through Virtual Reference Station (VRS) (Vollath et al., 2002) and Flächen korrektur parameter (FKP) (Wübbena and Bagge 2002) solution.

3. FIELD TEST

The user's receiver platform consisted of dual frequency receivers: Topcon GB1000 (GPS+GLONASS), JPSLegacy (GPS+GLONASS), Leica SR530 (GPS). The GB1000 and Leica SR530 receivers were used in real time NRTK-FKP and NRTK-VRS mode respectively. GSM devices were used to dial the computing control centre. The JPSLegacy receiver was set to log raw data for GPS+GLONASS post-processing purposes. A system of two antennae was located on the roof of a vehicle as shown in Figure 3. In order collect simultaneous observations with two receivers a splitter Model BT-2 was set to split the GNSS signal. Three testing combinations were designed for the user's receiver:

- Solution 1 - The GNSS signal of the antenna P1 was split to the Topcon GB1000 receiver for the NRTK - FKP solution and to the Leica SR530 for the VRS solution. A second antenna P2 was set to track a GPS+GLONASS signal for post processing purposes;

- Solution 2 - The GPS signal the antenna P1 was split to two receiver one working in real time the Topcon GB1000 in FKP solution and a second logging data for backup. A second antenna connected to Leica SR530 for the VRS solution.

- Solution 3 – Multi-kinematic post processed solutions of the antenna P1 and P2 using the subset of RS of Bologna (BOLO), Codigoro (COGO) and Ferrara (FERR) belonging to the BO-POS network.

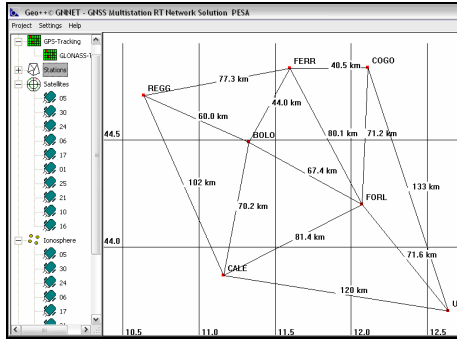


Figure 2. GNSMART software solution

GNSS NRTK correction were delivered using RTCM 2.3 format through message number 59 for the FKP and message number 18, 19, 20, 21 the VRS solutions. 5 degrees of cut off angle and 1 second sampling interval were chosen as *a priori* parameters for the kinematic test both for the users' receivers and for the RS..

Before starting the field survey a static session was planned to measure the distance between the phase centre of the antenna P1 and P2

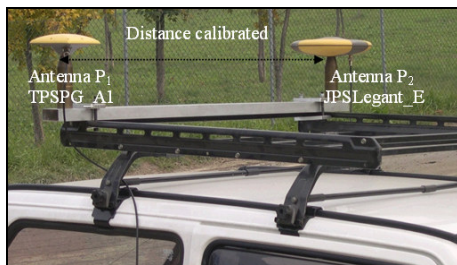


Figure 3. Double antennae equipped vehicle.

The kinematical testing trajectory length was about 40 km starting from Bologna University to Malalbergo near Ferrara (Figure 6).

4. THE RELIABILITY OF NRTK SOLUTIONS

The real time data were analysed to firstly evaluate the potentiality of the NRTK positioning in terms of availability and stability of the network solution. Figures 4 and 5 show the real time kinematical survey in terms of percentage of ambiguity resolved against the possible epochs tracked. In particular, Figure 4 shows results from session1 of the path from Bologna University to Malalbergo and back. A first sample of 5911 epochs was recorded with vehicle-average speed of 20÷30 km/h. A second sample of 3918 epochs was recorded on the way back with vehicle-average speed of 60÷70 km/h. Figure 4 shows that 33% of the possible epochs were float solutions; the

47 % were fixed solutions and the 20% code solutions when the speed was 20-30 km/h. The code solution is due to the absence of communication between the control centre and the rover receivers.

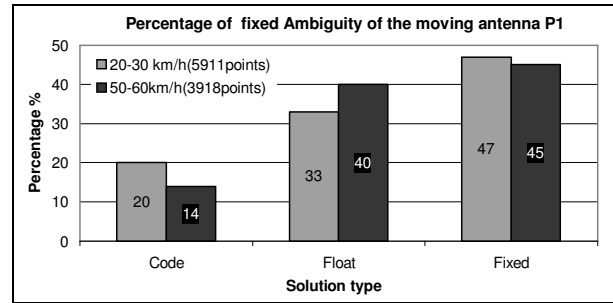


Figure 4. Session1 - Percentage of fixed ambiguity of antenna P1 in NRTK-FKP mode at different speed.

Figure 4 shows that the kinematic of the vehicle did not affect significantly the percentage of the fixed ambiguity. In fact the 47% of the possible epochs were fixed with 20÷30km/h speed against the 45% with 60÷70 km/h.

Figure 5 reports data from session2 and confirm results of Figure 4 in terms of percentage of fixed ambiguity resolved as an integer number with 41% of ambiguity solved in FKP mode and 59% in VRS mode with a sample of 9830 and 7568 of epochs respectively.

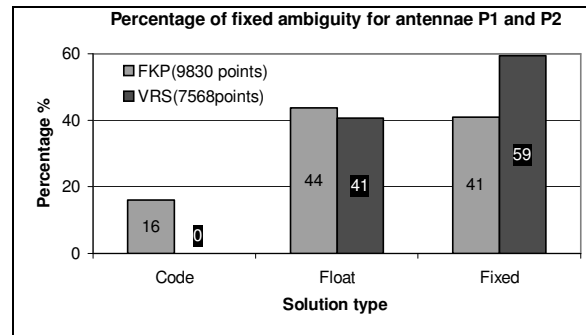


Figure 5. Session 2- Percentage of fixed solutions of antenna P1 and antenna P2 using FKP and VRS respectively. Average speed 60÷70km/h.

5. THE POST PROCESSED SOLUTIONS

Being the vehicle equipped with a double antenna system, six different trajectories could be computed with respect to the three RS chosen for the post processed solution. This configuration allowed to compute single baseline solutions for the antenna phase centres P1 and P2. Such post-processed solutions were computed using GeoGenius® 2000 and IGS precise orbits and relatively to data from session1. As shown in Figure 6 Bologna (BOLO), Ferrara (FERR) and Codigoro (COGO) RS named R1, R2 and R3 in the following sections, were used as master stations for the kinematic post processed solutions.

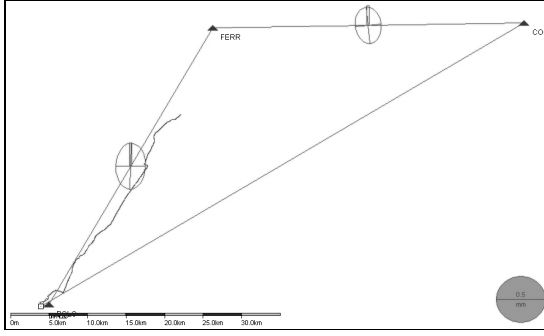


Figure 6. Single base station kinematic post-processing

The six autonomous single baseline kinematic solutions computed for the double antenna system give a sufficient degree of redundancy that allowed to build a tool capable of quality check for the final positioning. In fact this made possible to compute the inter-distance between the two roving antennae epoch by epoch and to constrain it to the calibrated distance. The discrepancies between the calibrated and the post processed intra-receiver distances that present values out of a fixed tolerance could be then detected and adjusted. The post processed solution did not evidence a clear correlation between the percentage of ambiguities fixed and distance between the base station and the moving antenna. Solutions R3-P2 (antenna P2 relatively to COGO base station) and R2-P1 (antenna P1 relatively to FERR base station) show the minimum number of ambiguities fixed.

Figure 7 show the discrepancies epoch by epoch between the calibrated distance (antenna P1 and P2) and the distance obtained from the post processing relatively to R1, R2 and R3 master stations in dark grey. As illustrated in the picture there are epochs with discrepancies up to 6 times the value of the calibrated distance, which refer to the DGPS solutions. This can be due with most probability to the poor satellite visibility and the effect of the multipath in correspondence of track passage on the road. In particular, the first epochs of the solutions correspond to the urban area of Bologna and the last epochs correspond to road track traffic.

Therefore this single baseline post processed solution is not accurate enough to be assumed as a reference trajectory to validate the network RTK positioning. For this reason a constrained adjustment was proposed to generate a more accurate post processed trajectory to be assumed as a touchstone for the following evaluations.

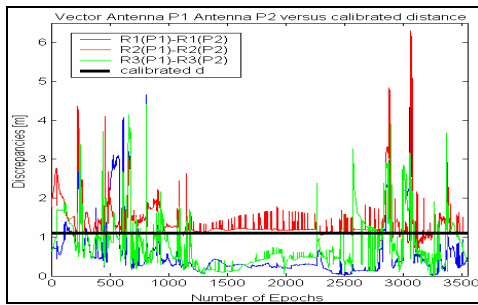


Figure 7. Single post processed solutions including DGPS and fixed solutions. 3-dimensional distance between antenna P1 and P2 versus calibrate distance d , data from session1.

6. 'MULTI-KIN' LEAST SQUARE-BASED SOLUTION

To increase the robustness of the kinematic post processed solution a least square adjustment-based method was implemented.

Such estimation was exerted over the post-processed kinematic solution carried out on each of the roving antennae with respect to the 3 Reference Stations (RS) considered in the test. The single baseline solution yields a path of the roving GPS receivers as the vehicle moves with respect to the RS chosen; thus, by selecting 3 RS, 6 observation equations can be written; three for each antenna.

From the observational point of view, the functional model exploits the coordinates stemming from the post processed kinematic as pseudo-observations into the estimation procedure; in fact considering the generic i -th roving antenna as observed through the j -th reference station, a typical vectorial equation can be written in terms of coordinates

$$\underline{x}^i - \tilde{x}_j^i = \underline{v} \quad (i=1, \dots, n; j=1, \dots, m) \quad (1)$$

where $\underline{x}^i = (x_1^i, x_2^i, x_3^i)$ is the coordinate vector of the i -th roving antenna, m is the number of the RS considered. Furthermore \tilde{x}_j^i are the coordinates of the i -th moving antenna that was observed from the j -th RS. Hence such a functional model will be composed by aggregating $m \cdot n \cdot 3$ scalar equations of the kind (1) and specialised as follows for this case ($m=3$ and $n=2$), with a block matrix notation:

$$\begin{bmatrix} \mathbf{I}_3 & \mathbf{0} \\ \mathbf{I}_3 & \mathbf{0} \\ \mathbf{I}_3 & \mathbf{0} \\ \mathbf{0} & \mathbf{I}_3 \\ \mathbf{0} & \mathbf{I}_3 \\ \mathbf{0} & \mathbf{I}_3 \end{bmatrix} \cdot \begin{bmatrix} \underline{x}_{3-1}^1 \\ \underline{x}_{3-1}^2 \end{bmatrix} = \begin{bmatrix} \underline{v}_{9-1}^1 \\ \underline{v}_{9-1}^2 \end{bmatrix} + \begin{bmatrix} \tilde{x}_{9-1}^1 \\ \tilde{x}_{9-1}^2 \end{bmatrix} \quad (2)$$

where \mathbf{I}_3 and $\mathbf{0}_3$ within the design matrix \mathbf{B}^* respectively defines the identity matrix of dimension 3, the Zero squared matrix of dimension 3, the partitioned column vector \underline{v}^i represents the misclosure's error for the functional model expressed by the (2). Such a model will be completed by adding further an observational equation which allows for the mutual distances between the two roving antennae; if the operator $\mathbf{d}: \mathbb{R}^3 \times \mathbb{R}^3 \rightarrow \mathbb{R}$ denotes the Euclidean distance in \mathbb{R}^3 , such an equation can be written with respect to the two roving antennae getting observations at the epoch t_h as follows:

$$\mathbf{d}(\underline{x}^i(t_h), \underline{x}^j(t_h)) - \tilde{\mathbf{d}} = v_d(t_h) \quad (3)$$

where, analogously, the term $\mathbf{d}(\underline{x}^i(t_h), \underline{x}^j(t_h))$ provides the theoretical distance between the two receivers at the epoch t_h issuing from the estimation procedure, whereas $\tilde{\mathbf{d}}$ refers to the same entity accurately measured; this equation needs to be linearized for the insertion into a least square estimation

procedure. Differentiating the equation (3) with respect to the the coordinates, one can get

$$\sum_{i=1}^3 (c_i^1) \delta x_i^1 + \sum_{k=1}^3 (c_k^2) \delta x_k^2 + d_0 - \tilde{d} = v_d(t_h) \quad (4)$$

where $c_i^j = \frac{\partial d}{\partial x_i^j}$ is the partial derivative coefficient computed

for the *a priori* value of the coordinates, $d_0 = \mathbf{d}(\underline{x}_0^i(t_h), \underline{x}_0^j(t_h))$ defines the *a priori* value of the intra-receiver distance computed at the epoch t_h and \tilde{d} represents the calibrated intra-receiver distance.

Geometrically speaking, Figure 8 displays the network topology, whose configuration changes epoch by epoch, as the vehicle moves: in fact it refers to a multiple trilaterated network, fully determined through a redundant number of baselines whose lengths shorten or lengthen according to the distance between the RS and the vehicle. The trilaterated scheme is further strengthened thanks to the vector connecting the two antennae. The datum defect of order 3 was worked out by fixing -throughout the least square estimation- the positions of the RS to their ITRF2000 values, arising from the BO-POS network solution performed by means of Bernese v5.0 Software; as such these estimations can be regarded as tightly constrained.

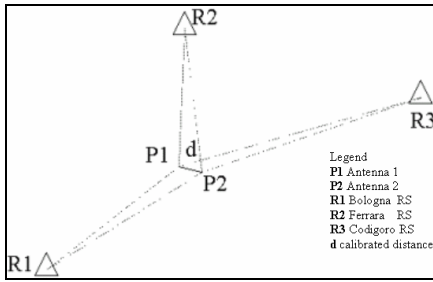


Figure 8. Scheme of the network configuration showing the connections among the Reference Stations and the Roving Antennae

Adding the distance equation to the functional model, the entire model needs to be linearized: nothing changes in the previous design matrix but the parameters to be estimated which are now differentials. The final functional model can be obtained for each epoch by concatenating the previous one, as synthesized by its design matrix, and the 6 elements row vector $\mathbf{c} = \begin{bmatrix} \mathbf{c}^i & \mathbf{c}^j \\ 1 & 3 \end{bmatrix}$ of the partial derivatives; finally, according to the following convention

$$\mathbf{B}^t = \begin{bmatrix} \mathbf{I}_3 & \mathbf{I}_3 & \mathbf{I}_3 & \mathbf{0} & \mathbf{0} & \mathbf{0} & (\mathbf{c}^i)^t \\ \mathbf{0} & \mathbf{0} & \mathbf{0} & \mathbf{I}_3 & \mathbf{I}_3 & \mathbf{I}_3 & (\mathbf{c}^j)^t \end{bmatrix} \quad (5)$$

the entire functional model can be finally expressed as follows:

$$\mathbf{B} \cdot \begin{bmatrix} \delta x_{3-1}^1 \\ \delta x_{3-1}^2 \end{bmatrix} + \begin{bmatrix} \mathbf{f} \\ f_d \end{bmatrix} = \begin{bmatrix} \mathbf{v} \\ v_d \end{bmatrix} \quad (6).$$

Such a linear system has to be coupled with a stochastic model, which characterizes the way all the observations are weighed into the estimation procedure. The formulation of this model imposes to blend different groups of observations -coordinates and distances- whose relative variances are assigned *a priori* through their variance-covariance (VCV) matrices. As regards this, a decomposition of the entire variance-covariance matrix is capable to better highlight the different observational contributions to the global VCV matrix. Let $\mathbf{D}(l)$ be the complete VCV matrix accounting for observations of coordinates and distances; according to block matrix notation one can get:

$$\mathbf{D}(l) = \text{diag}(\underbrace{\Sigma_{x_1^1}, \Sigma_{x_1^2}, \Sigma_{x_1^3}, \Sigma_{x_2^1}, \Sigma_{x_2^2}, \Sigma_{x_2^3}}_{19}, \underbrace{\sigma_d^2}_{1-1}) \quad (7)$$

which can be easily decomposed as follows:

$$\mathbf{D}(l) = \text{diag}(\underbrace{\Sigma_{x_1^1}, \Sigma_{x_1^2}, \Sigma_{x_1^3}, \Sigma_{x_2^1}, \Sigma_{x_2^2}, \Sigma_{x_2^3}}_{19}, 0) + \text{diag}(\underbrace{\mathbf{0}, \mathbf{0}, \mathbf{0}, \mathbf{0}, \mathbf{0}, \mathbf{0}}_{19}, \sigma_d^2) \quad (8)$$

where the first term in the summation is relevant to the coordinate observations and the second one to those of distance; moreover $\Sigma_{x_j^i}$ represents the 3-3 diagonal matrix pertaining to the variances of the *i*-th roving antenna with respect to the *j*-th reference station and the σ_d^2 defines the variance referring to the observation of the intra-roving receivers distance. The choice of the $\Sigma_{x_j^i}$ structure will characterize the stochastic model which is, at some extent, empirically formulated since it relies on the fact that, as the distances between the roving antennae and the established reference stations augment, the presence of mismodelled systematic errors tends to increase, thus making the classical RTK solution more unstable. In this case, each of the diagonal terms of $\Sigma_{x_j^i}$ was expressed as directly proportional to the distance between the receiver and the reference station in such a way that the following relationship holds:

$$\Sigma_{x_j^i} = k \cdot \underbrace{d(\underline{x}^i, \underline{x}_j)}_{1-1} \cdot \mathbf{I}_3 \quad (9)$$

k defining in this case a proper variance factor for the coordinate observations. As such the following relation holds:

$$\mathbf{D}(l) = k \cdot \mathbf{Q}(l_c) + \mathbf{D}(l_d) \quad (10)$$

where $\mathbf{Q}(l_c)$ represents the cofactor matrix of the coordinate observations for such a stochastic model. Now the variance factor k plays the role of further an unknown within the least square procedure, along with the P1 and P2 coordinates. Hence, denoting respectively with $\mathbf{E}(l)$ and $\mathbf{D}(l)$ the operators *expected value* and the *dispersion matrix* of the observations, the least square problem can be suitably formulated as follows:

$$\begin{cases} \mathbf{E}(l) = \mathbf{B}_{19,6} \cdot [\delta_{3,1}^1 & \delta_{3,1}^2]^t \\ \mathbf{D}(l) = k \cdot \mathbf{Q}_{19}(l_c) + \mathbf{D}_{19}(l_d) \end{cases} \quad (11)$$

In this model we're going to consider all the observations stochastically uncorrelated: that makes the matrix $\mathbf{D}(l)$ completely diagonal.

A suitable estimation of k can be reckoned solving a reduced least square problem which simply involves the coordinate observations and neglects the distances. Such a model -detailed at (2)- is stochastically homogeneous, thereby its solution is invariant under changes of the variance factor. Hence unbiased estimations of k will be computed epoch by epoch after having evaluated the quadratic form of the residuals relevant to the reduced problem as follows:

$$r \cdot k = \begin{bmatrix} \mathbf{V}_{1,9}^1 & \mathbf{V}_{1,9}^2 \end{bmatrix} \cdot \mathbf{P}_l \cdot \begin{bmatrix} \mathbf{V}_{9,1}^1 \\ \mathbf{V}_{9,1}^2 \end{bmatrix} \quad (12)$$

where r and \mathbf{P}_l are respectively the total redundancy and the weight matrix of the reduced least square problem whose diagonal terms are modelled as in (9).

As far as it is concerned, Figure 9 shows in blue the temporal variations of k as the network topology varies while the vehicle is moving.

Values of the variance factor k can be used as input to the complete model at (11) in order to balance the relative variances among the different observations

Normal matrix for the complete model formulated at (11) can be formally written in terms of weight matrix as follows:

$$\mathbf{P}(l) = \text{diag}(\mathbf{P}_{x_1}, \mathbf{P}_{x_2}, \mathbf{P}_{x_3}, \mathbf{P}_{x_1}, \mathbf{P}_{x_2}, \mathbf{P}_{x_3}, p_d^2) \quad (13)$$

where, as usual, the diagonal terms are all block diagonal matrix of dimension 3 except for the last scalar one

$$\begin{aligned} \mathbf{N} &= \mathbf{B}^t \cdot \mathbf{P} \cdot \mathbf{B} = \\ &= \begin{bmatrix} \mathbf{P}_{x_1} + \mathbf{P}_{x_2} + \mathbf{P}_{x_3} + p_d^2 (\mathbf{c}^i)^t \cdot (\mathbf{c}^j) & p_d^2 (\mathbf{c}^i)^t \cdot (\mathbf{c}^j) \\ p_d^2 (\mathbf{c}^j)^t \cdot (\mathbf{c}^i) & \mathbf{P}_{x_1} + \mathbf{P}_{x_2} + \mathbf{P}_{x_3} + p_d^2 (\mathbf{c}^j)^t \cdot (\mathbf{c}^j) \end{bmatrix} \end{aligned} \quad (14)$$

Analogously the right-hand side term of the normal equations in a least square sense gives

$$\begin{aligned} \mathbf{B}^t \cdot \mathbf{P} \cdot \mathbf{f} &= \\ &= \begin{bmatrix} \mathbf{P}_{x_1} \cdot \mathbf{f}(1; 3,1) + \mathbf{P}_{x_2} \cdot \mathbf{f}(4; 6,1) + \mathbf{P}_{x_3} \cdot \mathbf{f}(7; 9,1) + f_d p_d (\mathbf{c}^i)^t \\ \mathbf{P}_{x_1} \cdot \mathbf{f}(10; 12,1) + \mathbf{P}_{x_2} \cdot \mathbf{f}(13; 15,1) + \mathbf{P}_{x_3} \cdot \mathbf{f}(16; 18,1) + f_d p_d (\mathbf{c}^j)^t \end{bmatrix} \end{aligned} \quad (15)$$

Solutions to the least square problem can be get inverting the normal matrix at (14), thus providing the antennae positions P1

and P2 directly inserted into a global frame. As regards the solutions, Figure 9 displays in red the *a posteriori* intra-receiver distances, whose behaviour testifies the capability of the approach to adjust the relative positions of the double antenna system as the vehicle moves; in black it is superimposed the calibrated distance between the antennae. As evident, apart the initial epochs and the last ones where the solution reveals itself as noisier, it shows a good fit to the measured values for the middle part. Some blunders in the *a posteriori* distances are evident as a consequence of some floating solutions or misfixed carrier phase ambiguities in the post-processed solutions.

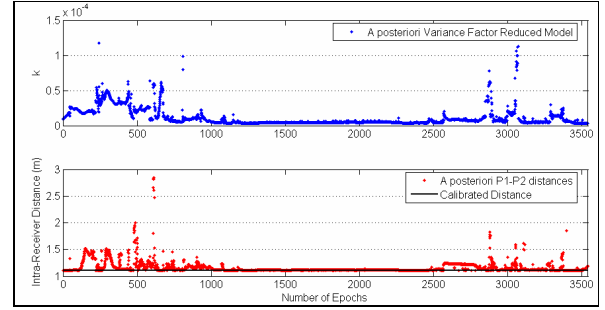


Figure 9. Synoptic view of the a posteriori variance factor for the reduced least square problem and Intra-Receiver Distances versus the number of epochs.

Synoptic view in Figure (9) testifies a certain correlation in the trends between the *a posteriori* variance factors k and the mutual distances: in fact higher values of distances somehow correspond to picks in the k factors; since the total redundancy factor remains unchanged throughout the entire estimations, such a behaviour testifies a corresponding increasing of the residuals in the quadratic form at (12) and , at the same time, a worst fit to the observational model. This Figure shows also the discrepancies between the adjusted and the calibrated P1-P2 distance using the 3544 common epochs; the multi-kin adjusted solution yields P1-P2 distance values which are much closer to the calibrated value; this behaviour is synthesized in Figure 10 by the histogram of the absolute values of the differences.

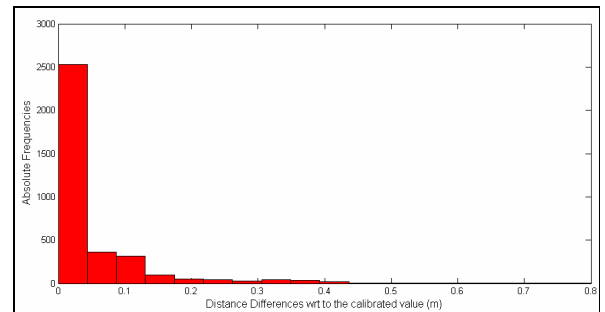


Figure 10. Histogram of the absolute frequencies for the quantity $(d(P1,P2)-\text{calibrated distance})$

The following figure provides, on the contrary, information about the displacement applied to the positions of P1 owing to the adjustment; a superimposition is here displayed between two quantities:

- the differences between the mutual distances between P1 and P2 as “observed” with respect to the farther Reference Station R3 and the calibrated value;

- the spherical errors δ between the solution P1 and the a priori positions of the same antenna as “observed” with respect to the Reference Station R3,

where δ formally indicates:

$$\delta = \sqrt{(\hat{x}_3^1 - \tilde{x}_3^1)^2 + (\hat{x}_2^1 - \tilde{x}_2^1)^2 + (\hat{x}_3^1 - \tilde{x}_3^1)^2} \quad (16).$$

As testified by the Figure 11, a certain correlation exists between the two diagrams: extreme blue values show mutual distances far from the calibrated one; such picks often corresponds to those in red values (δ), thus proving the effect of absolute correction applied to the P1 antenna points; same results hold for the antenna P2.

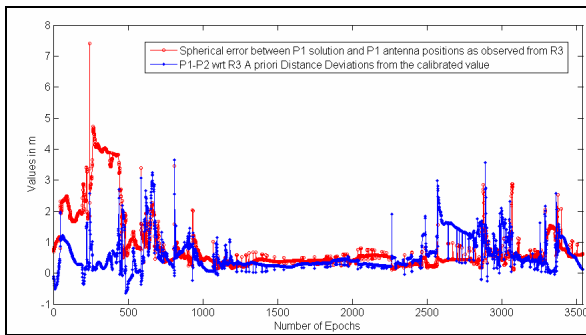


Figure 11. Correction entity applied to the P1 wrt R3 (in red) owing to the adjustment and errors in P1-P2 distance wrt R3 (in blue)

Figure 12 represents an example of adjusted position in red for the antenna 1 and 2 against the position obtained with GPS post processing relatively to the base station R1. A significant improvement of the adjusted solution is proved in relative (distance P1 and P2) and absolute (in term of position of antenna P1 and P1) terms.

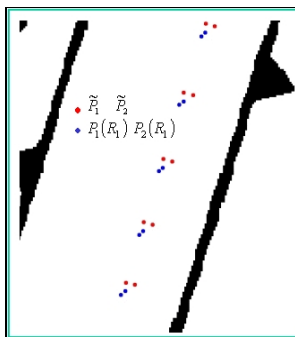


Figure 12. Example of adjusted solution in red and single base solution in blue. Cartography CTR 1:5000

The positions obtained by the adjustment will be assumed as a touchstone and used to validate the accuracy of NRTK positioning.

7. NRTK DATA VALIDATION

This section refers to data collected in session 1, suitably designed in order to evaluate the reliability and the accuracy of the NRTK positioning. In particular, the signal from antenna P1 (TPSPGA1 model) that was sent to the Topcon GB1000 receiver capable of NRTK-FKP positioning is here analysed.

In this section data of antenna 1 and antenna 2 multi-kin post adjusted are used to validate the accuracy of the NRTK data of antenna 1. In particular only the common epochs between the multi-kin adjusted and the NRTK-FKP solutions were selected, for a total amount of 1958 data.

In order to illustrate the difference between the NRTK and the adjusted solution one can consider the distance computed between the coordinates of P1 with an NRTK-FKP approach and those of P2 coming from the multi-kin adjustment. This value is showed in green in Figure 13; in red shown are the differences between the calibrated distance and that computed as (P1(NRTK)-P2(multi-adjusted)).

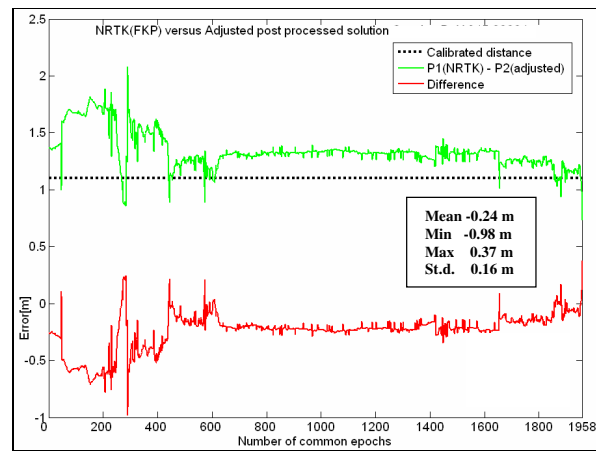


Figure 13. Difference between post processed adjusted solution and NRTK solutions in FKP mode.

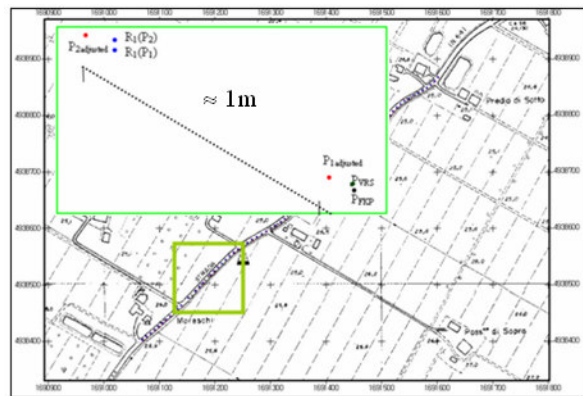


Figure 14. Adjusted and NRTK solution. Cartography CTR 1:5000

As clearly showed, the difference between multi-kin and NRTK solutions can attain metric level for the epochs corresponding to the trajectory in the Bologna urban area as a consequence of very poor satellite geometry; subsequently such difference tends to stabilise around 20 cm.

The figure 14 displays the good agreement of the trajectory suitably transformed into the National Cartographic System with the technical map at scale 1:5000.

8. CONCLUSIONS

This study proved the availability of the real time positioning of a vehicle within an area entirely covered by an NRTK service.

Unless the classical RTK procedures, such an approach does not ask for master stations along the vehicle's trajectory. Of course it has not been always possible to fix the phase ambiguities especially in urban areas, with a poor satellite visibility or in conditions of heavy traffic.

The use of two antennae, whose distance was measured and kept fixed, represents a valuable tool for selecting acceptable real time solutions.

A multi-kinematic method based on least square adjustment has been realized; the method shows the possibility to generate a very accurate solution to use as a reference trajectory to validate the positional accuracy of GNSS NRTK data. Data required for these computations are simply retrieved from the Continuously Operating Reference Stations in a such a way that they don't require further field efforts.

The results obtained for a 40 km trajectory highlighted the possibility to use NRTK for precise mobile mapping applications in agreement with large scale maps.

References from Journals:

Barbarella M. and Gordini C. (2005), Kinematic GPS Survey as Validation of LIDAR Strips Accuracy, *Annals of Geophysics* ISSN 0365-2556.

References from other Literature:

Al-Bayari O., (2000), 'Some Problems in Kinematic Airborne Laser Survey', Reports on Geodesy 6th Geodetic Millennium Meeting Poland-Italy.

Baldi P., Marsella M. e Vittuari L., (1998), 'Airborne GPS Performance during a photogrammetric project', *International Association of Geodesy Symposia*, Vol. 118 Brunner (ed.) *Advances in Positioning and Reference Frames*

Barbarella M., Gandolfi S. and Ronci E., (2006), 'The use of a GNSS Test Network for Real Time Application in Italy: First Results Based on Regional Field Test. Ion GNSS 19th International Technical Meeting of the Satellite Division, 26-29 September 2006, Forth Worth, TX

Barbarella M., Gandolfi S., Gordini C. e Vittuari L., (2003), 'Reti di stazioni permanenti per il posizionamento in tempo reale: prime sperimentazioni', *Atti della 7^o Conferenza Nazionale ASITA*, Verona 28-31 ottobre 2003, 173-178.

Gordini C., Kealy A., Grgich P., Hale M., 'A performance analysis of sparse GNSS CORS network for real Time Centimetric level Positioning: a case study in Victoria, Australia'. The 19th International Technical Meeting of the Institution of Navigation Satellite division. ION GNSS 2006 September 26-29 Forth Worth, Texas.

Landau H., Vollath U. and Chen X., (2003), 'Virtual Reference Stations versus Broadcast Solutions in Network RTK – Advantages and Limitations, *Proceedings of GNSS' The European Navigation Conference*, Graz, Austria, April 22-25.

Rizos C. and Han S., (2002), 'Reference station network based RTK systems: Concepts and progress', 4th Int. Symp. On GPS/GNSS, Wuhan, P.R. China, 6-8 November.

Vollath U., Buecherl A., Landau H., Pagels C. and Wagner B., (2000), 'Multi-Base RTK using Virtual Reference Stations', *Proceeding of the ION-GPS 2000*, Salt Lake City, Utah.

Vollath U., Landau H. and Chen X., (2002), 'Network RTK versus Single Base RTK – Understanding the Error Characteristics', *Proceedings of the 15th International Technical Meeting of the Satellite Division of the Institute of Navigation*, Portland, Oregon, USA, September.

Wübbena G., Bagge A. and Schmitz M., (2001), 'Network-Based Techniques for RTK Applications', *Proceedings of GPS Symposium 2001, Japan Institute of Navigation*, Nov. 14-16, 2001, Tokyo, Japan, pages 53-65

Wübbena G., Bagge A., (2002), 'RTCM Message Type 59-FKP for transmission of FKP', *Geo++[®] white paper* Nr. 2002.01, Garbsen, 2002 April 17.

References from websites:

ICSM (2004). Inter-governmental committee on surveying and mapping standards and practices for control surveys SP1 version 1.6 2004.

Trimble Navigation Limited, (2001). Trimble Virtual Reference Station VRS. VRS brochure. (http://trl.trimble.com/docushare/dsweb/Get/Document-11464/VRS_brochure.pdf).

Acknowledgments

The authors would like to acknowledge GEOTOP Srl and Leica Geosystems Italy SPA that provide the software and the receivers for the experiments. Also the authors wish to thank the colleagues of the DISTART that participated to the field session, in particular Dr. Alessandro Bedin.